

## Chaos Healing by Separatrix Disappearance and Quasisingle Helicity States of the Reversed Field Pinch

D. F. Escande,<sup>1,3</sup> R. Paccagnella,<sup>1,2</sup> S. Cappello,<sup>1,2</sup> C. Marchetto,<sup>1</sup> and F. D'Angelo<sup>1</sup>

<sup>1</sup>*Consorzio RFX, Corso Stati Uniti 4, 35127 Padova, Italy*

<sup>2</sup>*Consiglio Nazionale delle Ricerche, Rome, Italy*

<sup>3</sup>*UMR6633 CNRS-Universit e de Provence, Avenue Normandie-Niemen, 13397 Marseille Cedex 20, France*

(Received 22 March 2000)

The resilience to chaotic perturbations of one-parameter one-degree-of-freedom Hamiltonian dynamics is shown to increase when its corresponding separatrix vanishes due to a saddle-node bifurcation. This is first highlighted for the magnetic chaos related to quasisingle helicity (QSH) states of the reversed field pinch. It provides a rationale for the confinement improvement of helical structures experimentally found for QSH plasmas; such a feature would not be expected from the classical resonance overlap picture as the separatrix disappearance occurs when the amplitude of the dominant mode increases.

PACS numbers: 52.25.Fi, 52.30.Jb, 52.35.Ra, 52.55.Hc

This paper deals with two different, but connected issues: (i) the increase of the resilience to chaotic perturbations of a one-parameter one-degree-of-freedom Hamiltonian dynamics when its corresponding separatrix vanishes due to a saddle-node bifurcation, and (ii) a rationale for the confinement improvement experimentally found for helical domains in reversed field pinches in a quasisingle helicity (QSH) state [1]. Accordingly, this Letter is written so as to provide new results of interest for studies on magnetically confined plasmas and Hamiltonian chaos.

The reversed field pinch (RFP) is a toroidal magnetic confinement device similar to the tokamak but with a toroidal field,  $B_\phi$ , which reverses at the plasma edge, and which is of the same order of magnitude as the poloidal one,  $B_\theta$ . Let  $r$  measure the distance to the secondary magnetic axis of the torus, and  $R$  be its major radius. As the safety factor  $q = rB_\phi/RB_\theta$  is less than one, the plasma may easily become unstable to (resistive) kink modes. When such a mode resonates with the axisymmetric component of the magnetic field, it yields a magnetic island (if its amplitude is not too high, as will be shown later). In most experimental conditions, several such modes are simultaneously present with similar amplitudes of the order of a few percent of the axisymmetric magnetic field; such plasma states are dubbed multiple helicity (MH) states. Owing to the close mode spacing, this produces magnetic chaos in the plasma core [2] by resonance overlap [3]. Soft x-ray (SXR) tomographic measurements of MH states performed in RFX, the largest present RFP, show a rather axisymmetric thermal structure with its hottest point at the secondary axis of the plasma annulus [1].

In some experimental conditions, these tomographic measurements show the presence of a well defined thermal structure with  $m = 1$  poloidal symmetry [1]. These measurements correlate with external magnetic measurements which show a corresponding dominant mode; such plasma states are dubbed QSH states. However, the amplitudes of the nondominant magnetic modes stay often of the same

order of magnitude as in the MH state, and the simple resonance overlap picture predicts the island of the dominant mode to be chaotic, which is not compatible with the bright  $m = 1$  structures seen tomographically. This Letter provides a possible explanation to this apparently paradoxical situation, based on the absence of a magnetic separatrix for the dominant  $m = 1$  mode.

Numerical simulations of the RFP by 3D resistive magnetohydrodynamics codes also display MH and QSH states, and indicate the existence of a bifurcation between these states ruled by dissipation [4–8]. The 2D simulations of pure single helicity (SH) states show the existence of two topologies for the corresponding magnetic surfaces: with or without a magnetic separatrix, i.e., partially or fully reconnected magnetic field [9–12]. Figure 1 shows the typical poloidal section of the magnetic surfaces related to these two topologies. Figure 1(a) displays a large magnetic island which repels the magnetic axis existing in the unperturbed axisymmetric configuration. For a low amplitude of the helical magnetic mode, the O and X points of the island (points O' and X of the figure) lie close to the unperturbed circular resonant magnetic surface. In Fig. 1(b) there is no separatrix, but a helically distorted magnetic axis. The same two magnetic topologies are present in numerical simulations of the  $m = 1$  mode of the tokamak [13].

The QSH states of the RFP can be described by adopting the classical approximation of the plasma annulus by a straight cylinder. We use the usual cylindrical coordinates  $(r, \theta, z)$  and we follow the description of the magnetic field presented in [6]. The vector potential may be written as  $\mathbf{A} = \psi \nabla z + \Phi \nabla \theta$  with the gauge condition  $A_r = 0$ , where  $\psi$  and  $\Phi$  are the poloidal and toroidal fluxes, respectively. Then the magnetic field is of the form  $\mathbf{B} = \nabla \psi \times \nabla z + \nabla \Phi \times \nabla \theta$ . In the following we will be interested in the perturbation of a SH state where all quantities depend only on the two variables  $r$  and the helical angle  $u = m\theta + kz$  (we take  $m = 1$ );  $k$  plays the role of a toroidal mode number:  $k = -n_0/R$  where  $R$  is the

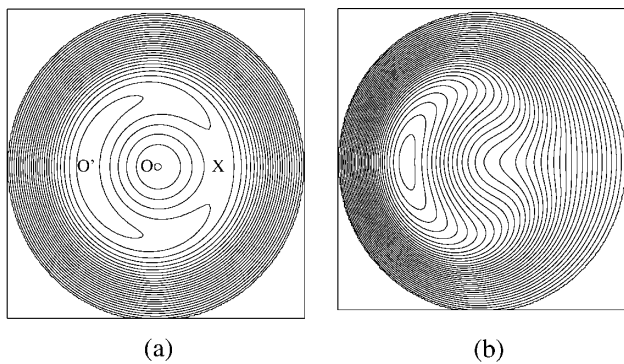


FIG. 1. Poloidal section of the magnetic flux surfaces of a single helicity plasma (a) with and (b) without a magnetic island.

major radius. By introducing the corresponding helical flux  $\chi = m\psi - k\Phi$ ,  $\mathbf{B}$  may be written

$$\mathbf{B} = (\nabla\psi \times \nabla u - \nabla\chi \times \nabla\theta)/k \quad (1)$$

(this is also correct without the helical symmetry). If  $\mathbf{A}$  depends only on  $r$  and  $u$ , calculating  $\mathbf{B} \cdot \nabla\chi$  from this equation one easily finds that  $\mathbf{B}$  is orthogonal to  $\nabla\chi$ , i.e., that  $\chi = \text{const}$  defines a magnetic surface. Therefore a SH state corresponds to an integrable magnetic field.

A Hamiltonian description of magnetic field lines enables the direct application of concepts and tools of Hamiltonian chaos to the magnetic field structure. Such a description is possible since the equations defining these lines can be cast as canonical equations of a Hamiltonian if one component of the magnetic field does not vanish in the domain of interest [14,15]. As  $B_\theta$  does not reverse in the RFP,  $\psi$  is single valued with respect to  $r$ .

Therefore  $\psi$ ,  $u$ , and  $\theta$  may be taken as independent variables. It is easily checked from Eq. (1) that  $\chi(\psi, u, \theta)$  is the required Hamiltonian [6], where  $\psi$  and  $u$  are the conjugate variables, and  $\theta$  plays the role of time. In the SH state  $\chi$  is independent of  $\theta$ , and is a one-degree-of-freedom Hamiltonian; therefore, as expected from the previous reasoning, it defines an integrable dynamics.

The numerically obtained QSH states show the presence of a dominant mode with  $m = 1$  and  $n = n_0$ , but other lower amplitude modes exist simultaneously [5,6,8]. Hence, chaos through resonance overlap [3] might happen. When an individual resonant magnetic mode ( $m, n$ ) with a small amplitude is present, the corresponding resonant magnetic surface, located at  $r = r_{m,n}$  such that  $q(r_{m,n}) = m/n$ , is torn into a small magnetic island whose width can be computed by a simple formula [3] valid in the tearing approximation, which is frequently used for  $m = 1$  modes in RFP data analysis; the result of this calculation is hereafter termed small amplitude island width (SAIW).

Figure 2 displays the safety factor  $q(r)$  of the axisymmetric part of the magnetic field of a QSH state with  $n_0 = 11$  computed by the SpeCyl code [5], together with horizontal bars showing the SAIW in  $r$  of a series of

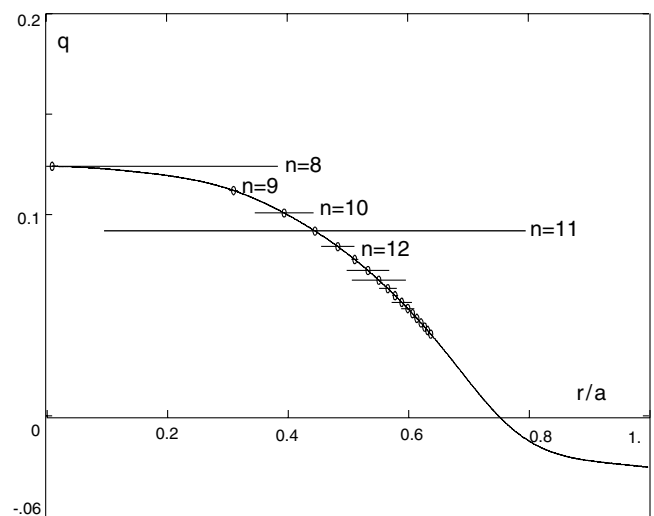


FIG. 2.  $q$  profile and magnetic islands width (shown by horizontal bars) of different  $m = 1$  modes.

$m = 1$  modes. We checked that the simple SAIW estimate is equal, within 30%, to the effective island width, as measured by direct reconstruction of the magnetic surfaces, except for the  $n = 8$  which is overestimated by a factor of 2. We see that the  $r$  domains of the bars have a strong overlap. This suggests the existence of large scale chaos everywhere in the width of the plasma. Figure 3(b) shows the Poincaré surface of section of the magnetic field lines in the plane ( $z, r$ ) obtained by computing these lines from the magnetic field of the same QSH state. Contrary to expectation, the system appears to be rather ordered: magnetic surfaces, or equivalently Kolmogorov-Arnold-Moser tori, still exist, although some limited chaotic regions are also present. In particular, the  $m = 1, n_0 = 11$  island structure of the dominant mode is clearly visible. Let  $\delta B$  be the amplitude of its magnetic field. An even more counterintuitive result is shown in Fig. 3(a) where the chaotic behavior of the magnetic field lines corresponds to a magnetic field of a new QSH state obtained by keeping the amplitude of all nondominant modes, but with a dominant mode amplitude  $\epsilon \delta B$  with  $\epsilon = 0.1$ . This corresponds to a decrease of magnetic island overlap, whereas chaos in the system increases.

We now show that the topological structure in phase space related to the dominant mode plays a crucial role in explaining the apparent paradox described above. Figure 1 displays the magnetic flux surfaces of the SH state obtained from the previous two QSH states by filtering out all modes except for the dominant one ( $m = 1, n_0 = 11$ ). Figure 1(a) corresponds to  $\epsilon = 0.1$  as in Fig. 3(a), while  $\epsilon = 1$  in Fig. 3(b) as in Fig. 3(b). While in case (a) there are two O points with a separatrix in between which yields a magnetic island, in case (b) there is only one O point and no magnetic island. Hence increasing  $\epsilon$  from 0.1 to 1, the system undergoes a topological change related to a saddle-node bifurcation (simultaneous bifurcation of an O point and of an X point): the small lobe of the separatrix

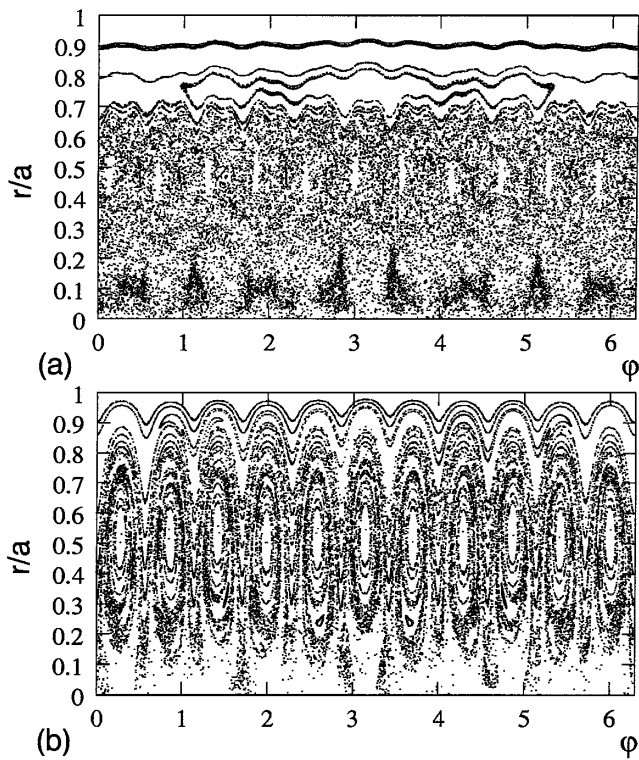


FIG. 3. Poincaré surface of section of magnetic field lines in the equatorial plane (a)  $\epsilon = 0.1$ , (b)  $\epsilon = 1$ .

in Fig. 1(a) shrinks to zero; this creates a cusp on the ultimate separatrix which then vanishes.

In order to explain why this bifurcation occurs when increasing  $\epsilon$ , and to understand its impact on chaos, we introduce a model for the helical flux

$$\chi_*(r, u) = \chi_0(r) + \epsilon \chi_1(r) \cos(u), \quad (2)$$

where  $\chi_0(r) = r^2 - ar^4$ , and  $\chi_1(r) = r(1 + br^2 - cr^4)$  with  $a$ ,  $b$ , and  $c$  positive numbers.  $\chi_0$  and  $\chi_1$  are the axisymmetric and first harmonics of the helical flux function. For an appropriate choice of  $(a, b, c)$  these first two components yield a good approximation of the full Fourier series for the magnetic field of Fig. 3(b) where  $\epsilon = 1$ , and  $\chi_* = \text{const}$  corresponds to the curves in Fig. 1.

The O and X points of Fig. 1 correspond to extrema of  $\chi_*$ , and are points where the magnetic field is purely helical with the helicity of the chosen SH state; indeed,  $\nabla u \cdot \mathbf{B} = -(\partial \chi_*/\partial r)/r$ . The function  $\chi_0(r)$  has a minimum at  $r = 0$  and a maximum at  $r = r_m = (2a)^{-1/2}$  separated by an inflection point at  $r = r_i = (6a)^{-1/2}$ . For  $\epsilon$  small (case of a tearing mode) one extremum of  $\chi$  is found at  $r = r_1$  close to  $r = 0$  with  $u = \pi$  and two extrema are found next to  $r = r_{1,11}$ , and symmetrically with respect to  $r_{1,11}$ , at  $r = r_2 > r_{1,11} > r_1$  with  $u = \pi$  and  $r = r_3 > r_2$  with  $u = 0$ . The analysis of the matrix of second derivatives shows that the points with respective index 1, 2, and 3 are, respectively, O, X, and O points [points O, X, and O' in Fig. 1(a)]. The first one corresponds to the kink of the magnetic axis at  $r = 0$  due to the finite value of  $\epsilon$ . The two

other ones correspond to the X and O points of the small magnetic island due to the tearing of the magnetic surface located at  $r = r_s$  for  $\epsilon$  small. Their order in radial position still holds for the  $\epsilon = 0.1$  value of Fig. 1(a), but the island is already broad, and the former  $r = 0$  magnetic axis is close to the X point. When  $\epsilon$  increases,  $r_1$  and  $r_2$  converge toward  $r_i$  and annihilate there for some critical value of  $\epsilon$  (saddle-node bifurcation). The vanishing of the X point corresponds to the disappearance of the related separatrix. For  $\epsilon = 1$  this already happened as shown in Fig. 1(b): no magnetic island exists, the magnetic surfaces are bean-shaped, a feature identical to that of the ideal kink; the new magnetic axis is the former O point of the island (the resonance is not removed). In numerical simulations of the SH state of the RFP starting from a paramagnetic pinch state to reach a fully reconnected magnetic field [12], the magnetic surfaces are seen to go through states with a separatrix before converging to a case without any. A similar dynamics was obtained in a simulation of the  $q = 1$  resistive kink in tokamaks [13].

Now that the change in the structure of phase space for the unperturbed motion is unveiled, the resilience of the fully reconnected SH state to chaos can be simply explained. Indeed, it is known that chaos develops in the vicinity of the separatrices of the unperturbed system, as a result of the homoclinic intersections [16] of the stable and unstable manifolds of the X point which merge in the unperturbed system. If a separatrix vanishes, so does the seed for chaos generation. We now make more quantitative this qualitative argument. To this end we use the formalism introduced above, and define  $\chi_H(\psi, u)$  as the Hamiltonian for the SH field lines related to  $\chi_*(r, u)$ . We then go to the action-angle variables  $(J, \phi)$  of this integrable system [6] which yields the Hamiltonian  $H_0(J)$ ; a flux surface then corresponds to  $J = \text{const}$ . When there is a separatrix, we do this in all three domains defined by the separatrix, and  $\Omega(J) = \partial H_0/\partial J$  vanishes at  $J_s$ , the corresponding value of  $J$ . If the SH state is perturbed by another helicity with  $m = 1$  and  $n = n_1$  of amplitude  $\eta$ , an appropriate choice of the origin of  $\theta$  enables one to write the corresponding Hamiltonian in the action angle as the following Fourier expansion

$$H(J, \phi, \theta) = H_0(J) + \eta \sum_{l=1}^{\infty} V_l(J) \cos(l\phi - \alpha\theta), \quad (3)$$

where  $\alpha = 1 - n_1/n_0$ . Since  $\Omega$  vanishes at  $J_s$ , the  $l$ th term of the Fourier expansion is resonant for  $l$  large enough, and we call it resonance  $l$ . As explained below, the resonance overlap criterion (ROC) may be used for Hamiltonian  $H$ . By using the universal expressions for action and frequency close to a separatrix [17], it is readily shown that the overlap parameter between resonance  $l$  and resonance  $l + 1$  scales like  $(\eta l \lambda^l)^{1/2}$ , where  $\lambda$  is a positive parameter which depends on  $H_0$ . Since  $\lambda$  is the unstable eigenvalue of the X point it is intrinsically greater than one. As a result chaos exists for any small positive value of  $\eta$  for  $l$  large enough. When  $\eta$  grows,

chaos expands away from the unperturbed separatrix. When the separatrix vanishes,  $\Omega(J)$  no longer vanishes, but has a positive minimum  $\Omega_m$  at some  $J = J_m$  close to  $J_s$ . The previous resonance overlap for any small  $\eta$  no longer holds. Chaos occurs close to  $J = J_m$  when  $\eta$  is large enough to allow the overlap of resonances  $l - 1$  and  $l$ , where  $l$  is the integer part of  $\alpha/\Omega_m$ . Therefore the disappearance of the separatrix implies a stronger resilience of the SH state to chaotic perturbations.

The features of Fig. 3(b) question the validity of the ROC. It is known that this criterion loses its validity when the overlapping islands have sufficiently different amplitudes or wavelengths [18]. Figure 2 shows that the dominant island has a SAIW such that it would overlap with neighboring islands even if they would have a vanishing amplitude: under such conditions the criterion is meaningless. A way out of this difficulty consists in the use of action-angle variables described above, which exhibits a set of new resonances. The features of neighboring resonances are similar enough, at least for large  $l$ 's, for the ROC to be applicable [19].

The argument based on action-angle variables does not depend on the details of the Hamiltonian system of interest. It shows that the impact of separatrix disappearance on the resilience to chaos is of general interest in Hamiltonian dynamics. It is interesting to notice that the growth of the amplitude of a given mode may produce a decrease of magnetic chaos in the corresponding resonant region even when the separatrix does not vanish. This is true for the stochastic layer which substitutes the separatrix for a small nonintegrable perturbation [19]. This is also true for a larger perturbation due to a quasiadiabatic behavior of the dynamics [20]. However, the absence of topological change in the dynamics makes the decrease of chaos more progressive.

We have shown that the resilience to chaos of a one-parameter one-degree-of-freedom Hamiltonian dynamics increases when its corresponding separatrix vanishes due to a saddle-node bifurcation. This was illustrated by the magnetic chaos related to QSH states of numerical simulations of the RFP. The similarity of experimental and numerical QSH spectra implies that the resonance overlap picture is likely to predict the absence of thermal structures with  $m = 1$  poloidal symmetry for QSH plasmas. Indeed, for such plasmas of RFX where a large hot helical structure is visible by SXR tomography, a preliminary application of the resonance overlap criterion to the data of external magnetic measurements predicts extended chaos where the helical structure is visible [21]. Chaos healing by separatrix disappearance might be the clue to this apparent paradox. The present development of internal measurements of magnetic field profiles will be important to check the experimental states against this theoretical picture.

The stronger resilience to chaos of a fully reconnected  $m = 1$  mode might also be important for the  $q = 1$  mode of the tokamak. Indeed, it was shown in Ref. [22] that

pressure induced chaos at the border of the  $q = 1$  island of a tokamak may increase heat transport and prevent the full Kadomtsev reconnection process occurring when the central  $q$  value,  $q_0$  is low enough (of order 0.8). As our theory shows that a fully reconnected  $q = 1$  mode is more resilient to Hamiltonian chaos, if the mechanism of Ref. [22] actually exists, one could expect transport at the inversion radius of soft x rays (radius of the  $q = 1$  mode) to decrease abruptly when  $q_0$  is increased from these low values toward 1 (but still less than 1).

The authors are indebted to Y. Elskens and S. Ortolani for useful comments on the manuscript and to F. Porcelli for advising them about the  $q = 1$  mode of the tokamak.

- 
- [1] P. Martin, *Plasma Phys. Controlled Fusion* **41**, A247 (1999); P. Martin *et al.*, *Phys. Plasmas* **7**, 1984 (2000).
  - [2] F. D'Angelo and R. Paccagnella, *Phys. Plasmas* **3**, 2353 (1996).
  - [3] B. Chirikov, *Phys. Rep.* **52**, 265 (1979).
  - [4] A. Sykes and J. Wesson, in *Proceedings of the 8th EPS Conference on Controlled Fusion and Plasma Physics, Prague, 1977* (European Physical Society, Prague, 1977), Vol. 1, p. 80.
  - [5] S. Cappello and R. Paccagnella, *Phys. Fluids B* **4**, 611 (1992).
  - [6] J.M. Finn, R. A. Nebel, and C. Bathke, *Phys. Fluids B* **4**, 1262 (1992).
  - [7] S. Cappello and D. Biskamp, *Nucl. Fusion* **36**, 571 (1996).
  - [8] S. Cappello, F. D'Angelo, D.F. Escande, R. Paccagnella, and D. Benisti, in *Proceedings of the 26th EPS Conference on Controlled Fusion and Plasma Physics, Maastricht, 1999* (European Physical Society, Bristol, U.K., 1999), Vol. 23J, p. 981.
  - [9] E.J. Caramana, R. A. Nebel, and D.D. Schnack, *Phys. Fluids* **26**, 1305 (1983).
  - [10] J. A. Holmes *et al.*, *Phys. Fluids* **28**, 261 (1985).
  - [11] D.D. Schnack, E.J. Caramana, and R. A. Nebel, *Phys. Fluids* **28**, 321 (1985).
  - [12] K. Kusano and T. Sato, *Nucl. Fusion* **26**, 1051 (1986).
  - [13] W. Park, D. A. Monticello, and R. B. White, *Phys. Fluids* **27**, 137 (1984).
  - [14] A. H. Boozer, *Phys. Fluids* **26**, 1288 (1983).
  - [15] F. Doveil, *J. Phys. (Paris)* **45**, 703 (1984).
  - [16] J. Guckenheimer and P. Holmes, *Nonlinear Oscillations, Dynamical Systems, and Bifurcations of Vector Fields* (Springer-Verlag, New York, 1986), p. 22.
  - [17] J.R. Cary, D. F. Escande, and J.L. Tennyson, *Phys. Rev. A* **34**, 4256 (1986).
  - [18] D.F. Escande and F. Doveil, *Phys. Lett.* **83A**, 307 (1981); *J. Stat. Phys.* **26**, 257 (1981); D.F. Escande, *Phys. Rep.* **121**, 165 (1985).
  - [19] D.F. Escande, *Physica (Amsterdam)* **6D**, 119 (1982).
  - [20] Y. Elskens and D.F. Escande, *Nonlinearity* **4**, 615 (1991); *Physica (Amsterdam)* **62D**, 66 (1993).
  - [21] D. Terranova (private communication).
  - [22] H. Baty, J.F. Luciani, and M.N. Bussac, *Phys. Fluids B* **5**, 1213 (1993).